A novel biotechnology based on periphytic biofilms with N-acyl-homoserine-lactones stimulation and lanthanum loading for phosphorus recovery

Ying Xu[a,b,c], Philip G. Kerr[d], Jan Dolfing[e], Bruce E. Rittmann[f], Yonghong Wu[a,b,g*]

[a] *State Key Laboratory of Soil and Sustainable Agriculture, Institute of Soil Science, Chinese Academy of Sciences, 71 East Beijing Road, Nanjing 210008, China*

[b] *Zigui Three Gorges Reservoir Ecosystem, Observation and Research Station of Ministry of Water Resources of the People's Republic of China, Shuitianba Zigui, Yichang 443605, China*

[c] *College of Resource and Environment, University of Chinese Academy of Sciences, Beijing 100049, China*

[d] *School of Biomedical Sciences, Charles Sturt University, Boorooma St, Wagga Wagga, NSW, 2678, Australia.*

[e] *Faculty of Energy and Environment, Northumbria University, Newcastle upon Tyne NE1 8QH, UK*

[f] *Biodesign Swette Center for Environmental Biotechnology, Arizona State University, P. O. Box 875701, Tempe, AZ 85287-5701, USA*

[g] *College of Hydraulic & Environmental Engineering, China Three Gorges University, Hubei Yichang 443002, China*

***Corresponding author**:

Dr. Yonghong Wu

E-mail: yhwu@issas.ac.cn (YW)

Telephone: (86)-25-8688 1330

Fax: (86)-25-8688 1000

Abstract

This study presents an approach for developing periphytic biofilm with N-acyl-homoserine-lactones (AHLs) stimulation and lanthanum (La, a rare earth element) loading, to achieve highly efficient and stable phosphorus (P) recovery from wastewater. AHLs stimulated biofilm growth and formation, also improved stable P entrapment by enhancing extracellular polymeric substance (EPS) production and optimizing P-entrapment bacterial communities. Periphytic biofilms loading La is based on ligand exchanges, and La loading achieved initial rapid P entrapment by surface adsorption. The combination of AHLs stimulation and La loading achieved 99.0% P entrapment. Interestingly, the enhanced EPS production stimulated by AHLs protected biofilms against La. Moreover, a method for P and La separately recovery from biofilms was developed, achieving 89-96% of P and 88-93% of La recovery. This study offers a promising biotechnology to reuse La from La-rich wastewater and recover P by biofilm doped with La, which results in a win-win situation for resource sustainability.

Keywords: Phosphorus recovery; Periphytic biofilm; N-acyl-homoserine-lactones; lanthanum loading

1. Introduction

The copious amounts of phosphorus (P) consumed in modern society (e.g., in foods and agricultural fertilizers) are eventually consolidated into wastewater (Cieślik & Konieczka, 2017). Wastewater must be recognized as a valuable P resource from which P can be harvested to produce energy and raw materials (Guest et al., 2009). Recovery of P from wastewaters before discharge is essential to mitigate negative environmental impacts and achieve economic P sustainability (Conley et al., 2009; Wang et al., 2015). P recovery using microbial communities is an ambitious yet promising "green" approach to enhance P sustainability (Chen et al., 2019; Wu et al., 2018; Zeng et al., 2021).

Periphytic biofilms are ubiquitous microbial aggregates in waters and are capable of entrapping P (Wu, 2016). The P entrapment mechanism of periphytic biofilm have been explored systematically to improve the recovery process. Two main processes dominate P recovery: extracellular and intracellular entrapment. Extracellular P entrapment is favored by a high content of extracellular polymeric substances (EPS), as functional groups such as NH_4^+ and mineral fractions such as Fe and Ca in the EPS are able to combine with P (Zhou et al., 2017). Intracellular P entrapment is carried out by a variety of P-entrapping microorganisms, especially those forming polyphosphate (Xu et al., 2020).

In periphytic biofilm, quorum sensing (QS), as a molecular communication system, relies on chemical signaling produced and transmitted by bacteria to direct and organize group behavior (Maddela et al., 2019). N-acyl homoserine lactones (AHLs), are the

main signal molecules used by the gram-negative bacteria prevailing in periphytic biofilms (Xu et al., 2020). AHLs-mediated QS has been shown to be closely related to EPS secretion, biofilm formation and P entrapment in periphytic biofilm (Lv et al., 2021; Xu et al., 2021). AHLs could regulate LysoPC metabolism that affects bacterial growth (Ma et al., 2018) and promotes EPS production by regulating the synthesis of amino acids and the UDP-Gal/UDP-Glc pathway (Tang et al., 2018b). In periphytic biofilm, AHLs addition up-regulated the genes involved in inorganic-P accumulation and P uptake (Xu et al., 2021). Thus, a strategy to promote P recovery through adjusting AHLs-mediated QS has been proposed.

Recently, lanthanum (La) has been used to develop P adsorbents, as it can enhance their rapid P adsorption capacity (Douglas et al., 2016). The 1-d P adsorption contents by La-modified bentonite were found to account for 86.4% of the 48-d adsorption in KH_2PO_4 solution (Haghseresht et al., 2009). The initial P entrapment rate of biofilms (0.5-1 mg $g^{-1}d^{-1}$) (Lu et al., 2016) is poor compared to chemical adsorbents (e.g., drinking water treatment residue: 2.42 mg $g^{-1}d^{-1}$) (Wang et al., 2018). Therefore, La offers hope for improving the rapid P entrapment of biofilms. The periphytic biofilm could in principle be modified by loading La from La-rich wastewater (e.g., tailings wastewater, La extraction wastewater), which also attains the recovery of La (Gavrilescu, 2021).

The proposed P recovery technology, based on periphytic biofilms, aims to exploit the potential synergistic benefits of AHL stimulation and La loading. In this process, it is envisaged that enhanced production of EPS as promoted by AHLs will result in the protection of microorganisms to withstand direct La exposure (Liu et al., 2019; Sun et

al., 2021). The La loaded on the biofilm will provide additional binding sites for rapid sequestration of P (Wang et al., 2018), while AHLs stimulates biofilm growth and aggregation which, in turn, can enhance the La loading capacity of the biofilm. To develop this novel technology, an insight in the loading process of La on periphytic biofilm and the combined effects of AHLs and La on P entrapment is required.

The studies can be divided into four phases.

i. Periphytic biofilm was modified by AHLs stimulation and La loading and the effects of AHLs and La on the physiological properties of the biofilm were investigated.

ii. Following the periphytic biofilm development, two simulated P wastewater removal experiments based on inorganic P and organic P were performed to evaluate P recovery by periphytic biofilm, as well as the advantages and possible synergistic effects of AHLs and La on P recovery.

iii. The loading mechanism of La on biofilms and the effect of La loading contents on the P recovery of biofilms were evaluated.

iv. A method was developed for the separate recovery of P and La from periphytic biofilms.

2. Materials and methods

2.1. Preparation of AHLs, La and periphytic biofilm

As described by Shaw et al (Shaw et al., 1997), AHLs were extracted from the supernatant of periphytic biofilm system. The main AHL signaling molecules from periphytic biofilms were determined, namely *N*-octanoyl-DL-homoserine lactone (C8-

HSL), *N*-(3-oxooctanoyl)-L-homoserine lactone (3OC8-HSL), *N*-dodecanoyl-DL-homoserine lactone (C12-HSL) (see supplementary materials). The synthetic AHLs (> 97%) were purchased from Sigma-Aldrich (Singapore): C8-HSL, 3OC8-HSL, C12-HSL.

Lanthanum (III) chloride ($LaCl_3$) (> 99.99%) were purchased (Sigma-Aldrich, Singapore).

Periphytic biofilm was collected from Xuanwu Lake, Nanjing, China and inoculated into culture systems containing Woods Hole culture medium (Xu et al., 2021). After about two weeks, the periphytic biofilm had matured - as indicated by a deep green color. Periphytic biofilms were collected and washed two times with sterile NaCl solution (0.9 %) and centrifuged before tests were run.

2.2. Periphytic biofilm with AHLs stimulation and La loading

An exogenous AHL mixture (C8-HSL, 3OC8-HSL, C12-HSL) was added to the periphytic biofilms system (biofilm concentration: 10 g /L wet weight), to yield a final AHLs concentration of 1 μM (for each AHL). Periphytic biofilms without added AHLs served as control. The systems were incubated under a standard light−dark cycle of 12 h/12 h (xenon lamp, 150 W) at 25 ± 1°C in a dedicated incubation room for 7d to obtain AHLs-stimulated periphytic biofilm.

The La loading by AHLs-stimulated periphytic biofilm was based on $LaCl_3$ solution. AHLs-stimulated periphytic biofilm (10 g/L) in conical flasks were supplemented with La solution (2 mg La/L); raw periphytic biofilm (without added AHLs) served as the La group. All tests were run in triplicate. After 24h of La loading, the periphytic biofilm

105 from, the AHLs-La and La groups were collected. The samples were snap-frozen with
106 liquid nitrogen and stored at −80 °C for subsequent analyses of the main structures and
107 the chemical compositions, EPS, biomass, enzymatic activities and community
108 composition.

109 *2.3. Characteristics of periphytic biofilm*

110 After AHLs stimulation and La loading, periphytic biofilms were sampled for growth
111 analysis based on the biomass. The main structures and the chemical compositions of
112 periphytic biofilms were characterized by scanning electron microscopy (SEM, JEOL
113 Co, Ltd., Japan) and energy dispersive X-ray spectroscopy (EDX, Oxford Instruments,
114 UK). The contents of La, Fe, Al, Ca, K, and Mg in periphytic biofilm were quantified
115 using inductively coupled plasma-atomic emission spectrometry (ICP-AES, Agilent
116 Technologies, Santa Clara, CA).

117 Enzymatic activities of periphytic biofilm, including adenosine triphosphatase
118 (ATPase), catalase (CAT), superoxide dismutase (SOD), acid phosphatase (ACP) and
119 alkaline phosphatase (AKP) were determined with enzyme assay kits (WST-1 method,
120 Jiancheng Bioengineering Institute, Nanjing, China). The diversity of the bacterial
121 communities in the biofilm matrix were analyzed by MiSeq sequencing technology
122 (Morales Sergio & Holben William, 2009). To study the P entrapment potential of the
123 community, the changes in the relative abundances of P-entrapment bacteria in the
124 different treatment groups were further analyzed.

125 *2.4. EPS analysis*

126 EPS were extracted from the periphytic biofilm with a sonication-cation exchange resin

method (Comte et al., 2006). The protein (PN) component of EPS was quantified by the coomassie brilliant blue staining method with bovine serum albumin as the standard (Frølund et al., 1995), whereas the polysaccharide (PS) component of EPS was determined using a phenol-sulfuric acid assay with glucose as the standard (Dubois et al., 1956).

The total contents of La, Fe, Al, Ca, K, and Mg in EPS were determined using ICP-AES. The chemical states of Al2p, Fe2p and C1s in EPS were determined by X-ray Photoelectron Spectroscopy (XPS, ESCALAB 250, Thermo Fisher Scientific, USA).

2.5. ROS accumulation of periphytic biofilm in the presence and absence of EPS

In the presence and absence of EPS, the generation of reactive oxygen species (ROS) induced by La loading was measured. After AHLs stimulation, periphytic biofilm (0.5 g wet weight) was put in conical flasks with La solution (100 mL, 5 mg La/L). To quantify ROS in the presence of EPS, biofilms were collected after 48h exposure. To quantify ROS in the absence of EPS, a heat treatment method (to avoid damaging biofilm cells) was used to removal EPS from periphytic biofilm prior to load La. In short, periphytic biofilm was collected, washed twice with 0.9% NaCl solution and centrifuged (10000 rpm, 10 min, 4 ˚C). Then the periphytic biofilm was resuspended with 0.9% NaCl solution and heated at 45 ˚C in a water bath for 30 min. All samples were centrifuged (10000 rpm, 10 min, 4 ˚C) to remove EPS from periphytic biofilm.

Previous studies have shown that limited heat treatment does not significantly affect ROS accumulation in periphytic biofilm (Fedyaeva et al., 2014; Li et al., 2018). The ROS were measured by reactive oxygen species Assay Kit method (100-500 T, Jiancheng Bioengineering Institute, Nanjing, China).

150 *2.6. P recovery test*

151 The P recovery tests included four groups, namely; (i) raw periphytic biofilm loaded
152 with La (La group) and (ii) not loaded (Control group), (iii) AHLs-stimulated periphytic
153 biofilm loaded with La (AHLs-La group) and (iv) not loaded with La (AHLs group).
154 The P recovery test was based on KH_2PO_4 and sodium glycerophosphate. Add 1 g (wet
155 weight) of periphytic biofilm into a conical flask containing 100 mL of 5 mg P/L
156 solution. In order to study the stability of P recovery by periphytic biofilms, the tests
157 were run for 30 days to observe whether the P would be released from the biofilm after
158 P recovery from the simulated wastewater. All tests were run in triplicate. pH in the
159 periphytic biofilm systems was also measured (pH-10, Sartorius, Germany). The
160 recovery tests were sampled regularly for P analysis. Total P analysis in solution was
161 determined by ICP-AES.

162 In order to study the relationship between the La-load on periphytic biofilms and their
163 P recovery capacity, the concentration of La in wastewater for the La loading test was
164 set to 0.5 (AHLs-0.5 La), 2 (AHLs-2 La), 5 (AHLs-5 La) and 10 (AHLs-10 La) mg
165 La/L. Samples of each were collected at the 24^{th} h for La loading content analysis. The
166 periphytic biofilms with different La loads were used for the P (H_2PO_4) recovery test.
167 P contents in periphytic biofilm were measured at 30d.

168 *2.7. P and La separately recovery processes*

169 A mixed solution of 3 % H_2SO_4 and 3 % HNO_3 were prepared. 1 g of periphytic biofilm
170 was placed in a polypropylene centrifuge tube and 10 mL of acid solution was added.
171 The mixtures were then sonicated (Ultrasonic cell disruptor; PS-60AL; Ldbsonic,

China) with 20% power, sonicated for 3 s at 10 s intervals, and repeated 30 times on ice. The biofilm was removed by centrifugation and La and P in the supernatant was separated by using a strong-acid cation exchange resin (Dowex 50X8; Dow Chemical Company, USA). A P-enriched solution and a La-enriched solution were obtained successively and P and La concentrations were measured using ICP-MS. The recovery efficiency was calculated based on the P entrapment amounts and REE loading amounts from ICP-MS data. The scheme of the recovery processes is illustrated in Fig. 1.

2.8. Statistical analysis

Statistically significant differences between the treatments and the controls were evaluated using ANOVA. For all analyses the significant *p*-value was set at 0.05. Pearson correlation between the EPS components and contents, and La loading capacity of EPS were evaluated using the package 'vegan' in R. The figures were drawn with Origin 9.0 and R software.

3. Results and discussion

3.1. P recovery by periphytic biofilm with AHLs stimulation and La loading

The P entrapment from simulated wastewater based on KH_2PO_4, is shown in Fig. 2a. La-loading substantially enhanced the initial entrapment by periphytic biofilms in comparison with non-La-loaded biofilms. According to the pseudo-second-order rate equation (see supplementary materials), from lowest to highest, the values were 0.63 mg $g^{-1}d^{-1}$ (Control), 1.59 mg $g^{-1}d^{-1}$ (AHLs), 6.07 mg $g^{-1}d^{-1}$ (La) and 7.52 mg $g^{-1}d^{-1}$

(AHLs-La). Initial P entrapment rates were substantially increased by pre-loading with La, while AHLs stimulation had less effect on the initial P-entrapment rate. After the 10th day, the P-entrapment content of periphytic biofilm in the AHLs-La group had reached 9.9 mg/g, i.e., 99% P-entrapment (Fig.2a). The P-entrapment of the La group had reached only 8.0 mg/g, i.e., 80% of the P-entrapment attained by the combination of La and AHLs. Moreover, the P-entrapment content by periphytic biofilm with AHLs-stimulation was found to steady at 9.9 mg/g over time until the 30th day, and the P concentration in wastewater had been below 0.1 mg/L. This indicated that the biofilm with AHLs-stimulation had a stable long-term P immobilization capacity, and it was difficult for P to be released into the wastewater again. Therefore, La-loading enhanced the rapid P-entrapment by periphytic biofilm, while AHLs stimulation tended to improve the stable P-entrapment.

For organic P wastewater, both AHLs and La promoted the entrapment of sodium glycerophosphate by the periphytic biofilms (Fig. 2b $p < 0.01$). P entrapment was further indicted by the observation that AHLs and La enhanced acid/alkaline phosphatase activity of the biofilms (Fig.6).

Whether it is inorganic P wastewater or difficult-to-treat organic P, the integration of AHLs-stimulation and La-loading has successfully improved the P recovery using periphytic biofilms, realizing the advantages of initial rapid P-entrapment, and steady and efficient P recovery. A method for P and La to be recovered separately from periphytic biofilms was developed; 88-92% of P and 87-91% of La can be recovered (Fig. 3), achieving sustainability of La and P.

3.2. *Relationship between La loading and P entrapment*

3.2.1. *La loading mechanism*

A large proportion of La loaded on the EPS, which indicated that EPS may be the main place for La loading (Table 1). The strong positive correlation between EPS production and La loading content supported this hypothesis (see supplementary materials). The chemical species of Al2p, Fe2p and C1s on EPS with and without La loading are shown in Table 1.

Al/Fe oxides increased with increasing La-loading, while a decrease in Al and Fe hydroxides were clearly observed. C in periphytic biofilm included aromatic C/C-C/C-H, C-O/aromatic C, C=O/ketone C, C in carboxylate groups, and C in carbonate groups. As La-loading increased, aromatic C/C-C/C-H (284.5–284.9 eV) and carboxylate groups (288.3 eV) tended to decrease, and C-O/aromatic C (286–286.3 eV) groups tended to increase. These results suggested the occurrence of ligand exchanges of La with the Al/Fe hydroxides and the carboxylate/phenol groups. La speciation is governed by the La ion hydrolysis. As pH was not regulated in this study and varied between 7.31-7.78, the dominant La species would be mostly La^{3+} with a small proportion of $LaOH^{2+}$; the existence of $La(OH)_2^+$, $La(OH)_3$ and $La(OH)_4^-$ is unlikely in this pH range (Bouyer et al., 2006). Thus, La loading into EPS was mainly based on ligand exchanges (equations (1)–(6)).

$$\equiv Al/Fe{-}OH + \equiv La{-}OH \rightarrow \equiv Al/Fe - O - La \equiv + H_2O \quad (1)$$

$$\equiv Al/Fe{-}OH + \equiv La \rightarrow \equiv Al/Fe - O - La \equiv + H^+ \quad (2)$$

$$RCOOH + \equiv La{-}OH \rightarrow RCOO - La \equiv + H_2O \quad (3)$$

$$RCOO^- + \equiv La \rightarrow RCOO - La \equiv \quad (4)$$

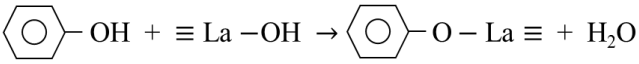

(5)

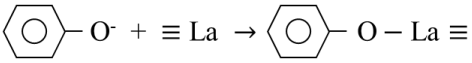

(6)

241 *3.2.2. La loading enhances rapid P entrapment*

242 The effect of pre-loading with La on P entrapment of periphytic biofilms is shown in
243 Fig. 2c and 2d. Initial P-entrapment clearly increased as the La load increased for
244 groups AHLs-0.5 La to AHLs-10 La ($p < 0.01$). In particular, the P-entrapment contents
245 rapidly increased to 9.9 mg g^{-1} in the AHLs-10 La group in which the initial P-
246 entrapment rate was up to 32.5 mg $g^{-1}d^{-1}$ (see supplementary materials). The results
247 indicated that enhanced initial P-entrapment occurs as the La load increases in
248 periphytic biofilm.

249 La have remarkably high binding affinities for P. La are able to combine with P, forming
250 $LaPO_4 \bullet nH_2O$, with a theoretical binding ratio between La and phosphate of 1:1 (Zhi
251 et al., 2020). In the simulated P wastewater, the dominant phosphate species at a pH
252 7.31-7.78 would be $H_2PO_4^-$ and HPO_4^-, as these are the only two species present at a
253 pH value of 5-10 (Li et al., 2020). Phosphate and La combined rapidly on the biofilm
254 surface, and the complex species can be inferred to be as follows (Zhi et al., 2020):

$$\equiv La + HPO_4^{2-} \rightarrow \equiv La - HPO_4 \quad (7)$$

$$\equiv La + H_2PO_4^- \rightarrow \equiv La - H_2PO_4 \quad (8)$$

257 *3.3. AHLs stimulation promotes biofilm growth and EPS production*

258 SEM indicated that a tight film and more substrate is present on the periphytic biofilm
259 surface after AHLs stimulation (see supplementary materials). The biofilm structure in

the control was observed to be looser and more porous. In the presence of AHLs for 7 days, the biomass of periphytic biofilm increased by 37%, whereas in the control group, the biomass increased by only 8% (Fig. 4a). These results suggested that the addition of AHLs accelerated the aggregation and growth of the periphytic biofilm (Técher et al., 2020; Zhang et al., 2020).

AHLs also substantially stimulated EPS production (Fig. 4b and c). Specifically, PN and PS content of EPS increased by 76.0 mg/g, and 12.7 mg/g, respectively, compared with the control ($p < 0.01$). This finding is in accordance with findings in previous studies in which supplementary QS signaling could increase EPS (Tang et al., 2018b). Previous studies have identified abundant functional groups (e.g., quaternary amines, tertiary amines) and mineral fractions (e.g., Mg^{2+}, Al^{3+}, Ca^{2+}, Fe^{3+}) in EPS, all of which can complex with phosphate-P (Zhou et al., 2017). The increase of EPS production induced by AHLs promoted extracellular P entrapment.

Periphytic biofilm with AHLs-stimulation contained more Fe, Al, Ca, K, and Mg ($p < 0.01$) than the control (Table 1). This may be due to the increased biomass and EPS content upon AHLs stimulation, which provided more binding sites for metal. However, La loading may reduce the metal adsorption capacity due to a dilution effect. As expected, total metal contents decreased in periphytic biofilm after La loading, suggesting that La loading reduced the metal adsorption capacity by occupying the adsorption sites (equations (1)–(6)).

3.4. Effect of AHLs and La on P-entrapment bacteria communities

The microbial composition of the biofilms changed dramatically upon AHLs-stimulation (Fig. 5a). In contrast, La had a relatively small effect on the biofilm community. In agreement with previous studies, periphytic biofilms in all four groups principally consisted of the phyla *Proteobacteria, Bacteroidetes, Cyanobacteria, Firmicutes,* and *Planctomycetes* (Tang et al., 2019; Wang et al., 2020). AHLs stimulation increased the abundance of the *Proteobacteria* phylum (51.7-52.7%) such that it became the most dominant phylum under AHLs stimulation, while a decrease in *Cyanobacteria.* Such a shift in the microbial community structure may be attributable to the fact that some genera under *Proteobacteria* favor the AHLs in study as their QS signaling for communication.

Further in-depth analysis (Fig. 5b) showed the effect of AHLs and La on the P-entrapment bacterial communities. Nine reported P-entrapment bacteria were found in biofilms, such as *Acinetobacter* (Deinema et al., 1980), *Pseudomonas* (Tobin Karen et al., 2007) and *Aeromonas* (Lotter & Murphy, 1985). They entrapped large quantities of P and stored it as polyphosphate. With AHLs-stimulation and La-loading, the relative abundances of P-entrapment bacteria were 12.92% (AHLs-La group), 9.76% (AHLs group), 1.46% (La group) and 1.93% (Control group). AHLs-stimulation resulted in a big increase in the abundance of P-entrapment bacteria, which indicated that AHLs can be used as a beneficial signal molecule for P-entrapment bacterial communities to improve the competitiveness of P-entrapment bacteria (Scott et al., 2017; Youk & Lim, 2014).

With no AHLs-stimulation, the La-loading led to a slight decrease in P-entrapment

304 bacteria abundance. While for AHLs-stimulated biofilms, La-loading had a significant
305 positive effect on P-entrapment bacterial communities.
306
307 *3.5.AHLs stimulation alleviates the adverse bioeffects of La loading*
308 The biological effects of La in periphytic biofilm were evaluated by measuring ATPase,
309 SOD and CAT activity (Fig. 6a). Microbial metabolic activity was represented by
310 ATPase activity, which increased substantially after AHLs stimulation ($p < 0.01$) (Liu
311 et al., 2018). The SOD activity is an indicator of oxidative stress caused by adverse
312 environmental conditions, and CAT alleviates damage caused by hydroxyl radicals (Xie
313 et al., 2019). For the periphytic biofilm without AHLs stimulation, the SOD and CAT
314 activity increased substantially with La loading ($p < 0.01$). Interestingly, an increased
315 SOD and CAT activity were not observed after AHLs stimulation, suggesting that AHLs
316 stimulation mitigated the stress induced by La and protected microbial cells in
317 periphytic biofilm.
318 In order to further explore the role of increased EPS productions caused by AHLs for
319 the stress protection, EPS scavenging tests were conducted. La exposure induced
320 adverse cell response: increased ROS levels. ROS prevalence substantially increased in
321 the absence of EPS compared to ROS prevalence in EPS containing biofilms (Fig. 6b,
322 $p < 0.01$), indicating that EPS can inhibit ROS prevalence. Moreover, in the presence
323 of EPS, AHLs stimulation alleviated ROS prevalence caused by La loading. After EPS
324 scavenging, no significant reduce of ROS prevalence was detected with AHLs
325 stimulation ($p > 0.05$). Therefore, enhanced production of EPS (Fig. 4b and c) caused

by AHLs-stimulation protected biofilms against La.

In the context of La loading, enhanced EPS production by AHLs stimulation has two benefits: to reduce or even eliminate direct La exposure on the periphytic biofilms thus providing sustainability for subsequent wastewater P recovery, and more importantly in this context, to provide a large number of binding sites that can load La (Li & Yu, 2014). EPS ineluctably influenced the distribution of La and their aggregation tendency which were important factors in their toxicity to microorganisms (Dang et al., 2018). With AHLs-stimulation, the elemental distribution investigation demonstrated that most La accumulated in the EPS (Table 1), which prevented La intrusion into the biofilm cells thus providing protection (Su et al., 2020). AHLs promoted EPS production and enhanced aggregation. The dense physical structure of the EPS acts as a barrier to La exposure in the interior of the periphytic biofilm. Aggregation also stabilizes microbial diversity, which enhance the ability of the community to adapt to La loading (Tang et al., 2018a).

Based on the results of the biological test and the P entrapment capacity of periphytic biofilm in aqueous solutions, AHLs stimulation and La loading on biofilms achieved P sustainability, and served to enhance the effectiveness of eutrophication control across a broad range of waters. Notably, La loading from La-rich wastewater also attained the La recovery.

4. Conclusions

This study proposed an innovative bioaugmentation strategy based on periphytic biofilm to achieve highly efficient and stable P recovery from wastewater. AHLs-

stimulation enhanced stable P-entrapment via increasing the EPS production and optimizing P-entrapment bacterial communities. La-loading achieved initial rapid P entrapment by improving surface adsorption. Periphytic biofilm loads La from La-rich wastewater and realizes the reuse of La. Periphytic biofilm with AHLs stimulation and La loading achieved 99.0% P entrapment. Moreover, AHLs stimulation alleviated the adverse bioeffects of La loading. Finally, 88-92% of P and 87-91% of La can be recovered from periphytic biofilms, achieving sustainability of P and La.

Acknowledgements

This work was supported by the National Natural Science Foundation of China (41825021, 41961144010 and 31772396), the Original Innovation Project of Chinese Academy of Sciences (ZDBS-LY-DQC024), and the Natural Science Foundation of Jiangsu Province, China (BZ2019015 and BE2020731).

Declaration of Competing Interest

The authors declare that they have no known competing financial interests or personal relationships that could have appeared to influence the work reported in this paper.

CRediT authorship contribution statement

Ying Xu: Investigation, Methodology, Visualization, Data curation, Formal analysis, Writing – original draft. **Philip Kerr**: Formal analysis, Writing - review & editing. **Jan Dolfing**: Formal analysis, Writing - review & editing. **Bruce Rittmann**: Conceptualization, Writing - review & editing. **Yonghong Wu**: Funding acquisition, Supervision, Conceptualization, Writing - review & editing.

Reference

1. Bouyer, F., Sanson, N., Destarac, M., Gérardin, C. 2006. Hydrophilic block copolymer-directed growth of lanthanum hydroxide nanoparticles. *New J. Chem.*, **30**(3), 399-408.
2. Chen, W., Mo, J., Du, X., Zhang, Z., Zhang, W. 2019. Biomimetic dynamic membrane for aquatic dye removal. *Water Res.*, **151**, 243-251.
3. Cieślik, B., Konieczka, P. 2017. A review of phosphorus recovery methods at various steps of wastewater treatment and sewage sludge management. The concept of "no solid waste generation" and analytical methods. *J. Clean Prod.*, **142**, 1728-1740.
4. Comte, S., Guibaud, G., Baudu, M. 2006. Relations between extraction protocols for activated sludge extracellular polymeric substances (EPS) and EPS complexation properties: Part I. Comparison of the efficiency of eight EPS extraction methods. *Enzyme Microb. Tech.*, **38**(1), 237-245.
5. Conley, D.J., Paerl, H.W., Howarth, R.W., Boesch, D.F., Seitzinger, S.P., Havens, K.E., Lancelot, C., Likens, G.E. 2009. Controlling eutrophication: nitrogen and phosphorus. *Science*, **323**(5917), 1014-1015.
6. Dang, C., Yang, Z., Liu, W., Du, P., Cui, F., He, K. 2018. Role of extracellular polymeric substances in biosorption of Pb^{2+} by a high metal ion tolerant fungal strain *Aspergillus niger* PTN31. *J. Environ. Chem. Eng.*, **6**(2), 2733-2742.
7. Deinema, M.H., Habets, L.H.A., Scholten, J., Turkstra, E., Webers, H.A.A.M. 1980. The accumulation of polyphosphate in *Acinetobacter* spp. *FEMS Microbiol. Lett.*, **9**(4), 275-279.
8. Douglas, G.B., Hamilton, D.P., Robb, M.S., Pan, G., Spears, B.M., Lurling, M. 2016. Guiding principles for the development and application of solid-phase phosphorus adsorbents for freshwater ecosystems. *Aquat. Ecol.*, **50**(3), 385-405.
9. Dubois, M., Gilles, K.A., Hamilton, J.K., Rebers, P.t., Smith, F. 1956. Colorimetric method for determination of sugars and related substances. *Anal. Chem.*, **28**(3), 350-356.
10. Fedyaeva, A.V., Stepanov, A.V., Lyubushkina, I.V., Pobezhimova, T.P., Rikhvanov, E.G. 2014. Heat shock induces production of reactive oxygen species and increases inner mitochondrial membrane potential in winter wheat cells. *Biochem. Mosc.*, **79**(11), 1202-1210.
11. Frølund, B., Griebe, T., Nielsen, P.H. 1995. Enzymatic activity in the activated-sludge floc matrix. *Appl. Microbiol. Biot.*, **43**(4), 755-761.
12. Gavrilescu, M. 2021. Microbial recovery of critical metals from secondary sources. *Bioresour. Technol.*, 126208.
13. Guest, J.S., Skerlos, S.J., Barnard, J.L., Beck, M.B., Daigger, G.T., Hilger, H., Jackson, S.J., Karvazy, K., Kelly, L., Macpherson, L., Mihelcic, J.R., Pramanik, A., Raskin, L., Van Loosdrecht, M.C.M., Yeh, D., Love, N.G. 2009. A new planning and design paradigm to achieve sustainable resource recovery from wastewater. *Environ. Sci. Technol.*, **43**(16), 6126-6130.
14. Haghseresht, F., Wang, S., Do, D.D. 2009. A novel lanthanum-modified bentonite, Phoslock, for phosphate removal from wastewaters. *Appl. Clay Sci.*, **46**(4), 369-375.

15. Li, H., Liu, Y., Gu, Z., Li, L., Liu, Y., Wang, L., Su, L. 2018. p38 MAPK-MK2 pathway regulates the heat-stress-induced accumulation of reactive oxygen species that mediates apoptotic cell death in glial cells. *Oncol. Lett.*, **15**(1), 775-782.
16. Li, W.-W., Yu, H.-Q. 2014. Insight into the roles of microbial extracellular polymer substances in metal biosorption. *Bioresour. Technol.*, **160**, 15-23.
17. Li, X., Chen, J., Zhang, Z., Kuang, Y., Yang, R., Wu, D. 2020. Interactions of phosphate and dissolved organic carbon with lanthanum modified bentonite: Implications for the inactivation of phosphorus in lakes. *Water Res.*, **181**, 115941.
18. Liu, J., Tang, J., Wan, J., Wu, C., Graham, B., Kerr, P.G., Wu, Y. 2019. Functional sustainability of periphytic biofilms in organic matter and Cu^{2+} removal during prolonged exposure to TiO_2 nanoparticles. *J. Hazard. Mater.*, **370**, 4-12.
19. Liu, J., Wang, M., Yi, H., Liu, M., Zhu, D., Wu, Y., Jia, R., Sun, K., Yang, Q., Chen, S., Zhao, X., Chen, X., Cheng, A. 2018. ATPase activity of GroEL is dependent on GroES and it is response for environmental stress in *Riemerella anatipestifer*. *Microb. Pathogenesis*, **121**, 51-58.
20. Lotter, L., Murphy, M. 1985. The identification of heterotrophic bacteria in an activated sludge plant with particular reference to polyphosphate accumulation. *Water SA*, **11**(4), 179-184.
21. Lu, H., Feng, Y., Wu, Y., Yang, L., Shao, H. 2016. Phototrophic periphyton techniques combine phosphorous removal and recovery for sustainable salt-soil zone. *Sci. Total Environ.*, **568**, 838-844.
22. Lv, L., Feng, C., Li, W., Zhang, G., Ren, Z., Liu, X., Song, X., Wang, P. 2021. Exogenous N-acyl-homoserine lactones accelerate resuscitation of starved anaerobic granular sludge after long-term stagnation. *Bioresour. Technol.*, **337**, 125362.
23. Ma, H., Wang, X., Zhang, Y., Hu, H., Ren, H., Geng, J., Ding, L. 2018. The diversity, distribution and function of N-acyl-homoserine lactone (AHL) in industrial anaerobic granular sludge. *Bioresour. Technol.*, **247**, 116-124.
24. Maddela, N.R., Sheng, B., Yuan, S., Zhou, Z., Villamar-Torres, R., Meng, F. 2019. Roles of quorum sensing in biological wastewater treatment: A critical review. *Chemosphere*, **221**, 616-629.
25. Morales Sergio, E., Holben William, E. 2009. Empirical testing of 16S rRNA gene PCR primer pairs reveals variance in target specificity and efficacy not suggested by In silico analysis. *Appl. Environ. Microbiol.*, **75**(9), 2677-2683.
26. Scott, S.R., Din, M.O., Bittihn, P., Xiong, L., Tsimring, L.S., Hasty, J. 2017. A stabilized microbial ecosystem of self-limiting bacteria using synthetic quorum-regulated lysis. *Nat. Microbiol.*, **2**(8), 17083.
27. Shaw, P.D., Ping, G., Daly, S.L., Cha, C., Cronan, J.E., Rinehart, K.L., Farrand, S.K. 1997. Detecting and characterizing N-acyl-homoserine lactone signal molecules by thin-layer chromatography. *PNAS*, **94**(12), 6036.
28. Su, H., Zhang, D., Antwi, P., Xiao, L., Liu, Z., Deng, X., Asumadu-Sakyi, A.B., Li, J. 2020.

Effects of heavy rare earth element (yttrium) on partial-nitritation process, bacterial activity and structure of responsible microbial communities. *Sci. Total Environ.*, **705**, 135797.

29. Sun, R., Xu, Y., Wu, Y., Tang, J., Esquivel-Elizondo, S., Kerr, P.G., Staddon, P.L., Liu, J. 2021. Functional sustainability of nutrient accumulation by periphytic biofilm under temperature fluctuations. *Environmen. Technol.*, **42**(8), 1145-1154.
30. Tang, C., Sun, P., Yang, J., Huang, Y., Wu, Y. 2019. Kinetics simulation of Cu and Cd removal and the microbial community adaptation in a periphytic biofilm reactor. *Bioresour. Technol.*, **276**, 199-203.
31. Tang, J., Wu, Y., Esquivel-Elizondo, S., Sørensen, S.J., Rittmann, B.E. 2018a. How microbial aggregates protect against nanoparticle toxicity. *Trends Biotechnol.*, **36**(11), 1171-1182.
32. Tang, X., Guo, Y., Wu, S., Chen, L., Tao, H., Liu, S. 2018b. Metabolomics uncovers the regulatory pathway of Acyl-homoserine lactones based quorum sensing in anammox consortia. *Environ. Sci. Technol.*, **52**(4), 2206-2216.
33. Técher, D., Grosjean, N., Sohm, B., Blaudez, D., Le Jean, M. 2020. Not merely noxious? Time-dependent hormesis and differential toxic effects systematically induced by rare earth elements in *Escherichia coli*. *Environ. Sci. Pollut. Res.*, **27**(5), 5640-5649.
34. Tobin Karen, M., McGrath John, W., Mullan, A., Quinn John, P., O'Connor Kevin, E. 2007. Polyphosphate accumulation by *Pseudomonas putida* CA-3 and other medium-chain-length polyhydroxyalkanoate-Accumulating Bacteria under Aerobic Growth Conditions. *Appl. Environ. Microbiol.*, **73**(4), 1383-1387.
35. Wang, C., Wu, Y., Wang, Y., Bai, L., Jiang, H., Yu, J. 2018. Lanthanum-modified drinking water treatment residue for initial rapid and long-term equilibrium phosphorus immobilization to control eutrophication. *Water Res.*, **137**, 173-183.
36. Wang, S., Ma, L., Xu, Y., Wang, Y., Zhu, N., Liu, J., Dolfing, J., Kerr, P., Wu, Y. 2020. The unexpected concentration-dependent response of periphytic biofilm during indole acetic acid removal. *Bioresour. Technol.*, **303**, 122922.
37. Wang, X., McCarty, P.L., Liu, J., Ren, N.-Q., Lee, D.-J., Yu, H.-Q., Qian, Y., Qu, J. 2015. Probabilistic evaluation of integrating resource recovery into wastewater treatment to improve environmental sustainability. *PNAS*, **112**(5), 1630.
38. Wu, Y. 2016. *Periphyton: functions and application in environmental remediation*. Elsevier.
39. Wu, Y., Liu, J., Rene, E.R. 2018. Periphytic biofilms: a promising nutrient utilization regulator in wetlands. *Bioresour. Technol.*, **248**, 44-48.
40. Xie, J., Zhao, L., Liu, K., Liu, W. 2019. Enantiomeric environmental behavior, oxidative stress and toxin release of harmful cyanobacteria *Microcystis aeruginosa* in response to napropamide and acetochlor. *Environ. Pollut.*, **246**, 728-733.
41. Xu, Y., Curtis, T., Dolfing, J., Wu, Y., Rittmann, B.E. 2021. N-acyl-homoserine-lactones signaling as a critical control point for phosphorus entrapment by multi-species microbial aggregates. *Water Res.*, **204**, 117627.
42. Xu, Y., Wu, Y., Esquivel-Elizondo, S., Dolfing, J., Rittmann, B.E. 2020. Using microbial

aggregates to entrap aqueous phosphorus. *Trends Biotechnol.*, **38**(11), 1292-1303.

43. Youk, H., Lim, W.A. 2014. Secreting and sensing the same molecule allows cells to achieve versatile social behaviors. *Science*, **343**(6171), 1242782.
44. Zeng, X., Huang, J.J., Hua, B. 2021. Efficient phosphorus removal by a novel halotolerant fungus *Aureobasidium* sp. MSP8 and the application potential in saline industrial wastewater treatment. *Bioresour. Technol.*, **334**, 125237.
45. Zhang, B., Li, W., Guo, Y., Zhang, Z., Shi, W., Cui, F., Lens, P.N.L., Tay, J.H. 2020. A sustainable strategy for effective regulation of aerobic granulation: Augmentation of the signaling molecule content by cultivating AHL-producing strains. *Water Res.*, **169**, 115193.
46. Zhi, Y., Zhang, C., Hjorth, R., Baun, A., Duckworth, O.W., Call, D.F., Knappe, D.R.U., Jones, J.L., Grieger, K. 2020. Emerging lanthanum (III)-containing materials for phosphate removal from water: A review towards future developments. *Environ. Int.*, **145**, 106115.
47. Zhou, Y., Nguyen, B.T., Zhou, C., Straka, L., Lai, Y.S., Xia, S., Rittmann, B.E. 2017. The distribution of phosphorus and its transformations during batch growth of *Synechocystis*. *Water Res.*, **122**, 355-362.

Figure captions

Figure 1. Dual process for recovery of P and La.

Figure 2. P entrapment performance of periphytic biofilms with AHLs-stimulation and La-loading. P entrapment by biofilms in wastewater based on (a) KH_2PO_4 and (b) sodium glycerophosphate. (c) La loading by AHL-stimulated periphytic biofilm in solutions with different La concentrations. (d) P entrapment by AHL-stimulated periphytic biofilm with different La contents loaded. PB: periphytic biofilm; **AHLs-La** represents periphytic biofilm with AHLs-stimulation and La-loading; **AHLs** represents periphytic biofilm with AHLs-stimulation; **La** represents raw periphytic biofilm with La-loading; **Control** represents raw periphytic biofilm. Symbols indicate means and error bars show the standard deviation for the replicates (n=3).

Figure 3. Recovery of P and La from periphytic biofilm. Symbols indicate means and error bars show the standard deviation of the replicates (n=4).

Figure 4. Effects of AHLs-stimulation on (a) biomass of periphytic biofilm, (b) protein (PN) and (c) polysaccharide (PS) in EPS. Symbols indicate means and error bars show the standard deviation of the replicates (n=3). ** and * indicate highly significant correlations ($p < 0.01$) and significant correlations ($p < 0.05$) respectively.

Figure 5. Effect of AHLs and La on microbial composition. (a) Community composition of bacteria at the phylum level, and (b) distribution of the P-entrapment bacteria in periphytic biofilm with AHLs-stimulation and La-loading.

Figure 6. Effect of AHLs and La on enzymatic activity and reactive oxygen species (ROS). (a) Effect of AHLs-stimulation and La-loading on enzymatic activity of periphytic biofilms. (b) In the presence or absence of EPS, the effect of La on the ROS accumulation in periphytic biofilms. Symbols indicate means and error bars show the

standard deviation of the replicates (n=3). ** and * indicate highly significant correlations ($p < 0.01$) and significant correlations ($p < 0.05$) respectively.

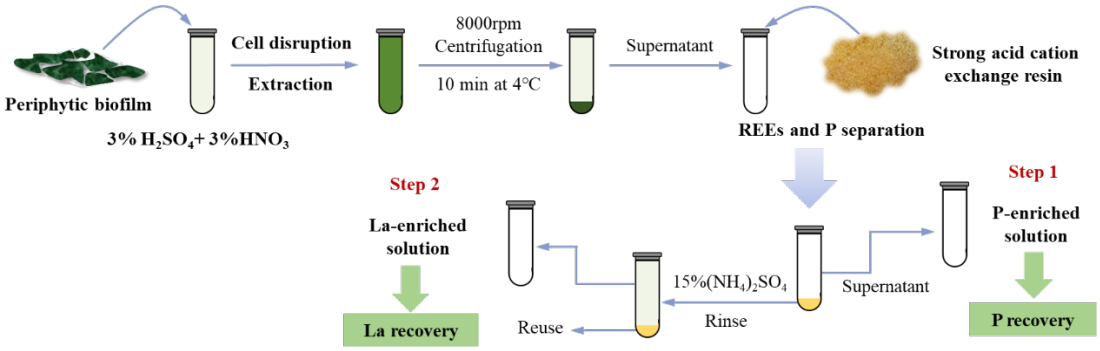
Periphytic biofilm
3% H_2SO_4+ 3%HNO_3
Cell disruption
Extraction
8000rpm
Centrifugation
10 min at 4°C
Supernatant
Strong acid cation exchange resin
REEs and P separation
Step 1
P-enriched solution
P recovery
Supernatant
15%$(NH_4)_2SO_4$
Rinse
Reuse
Step 2
La-enriched solution
La recovery

Figure 1.

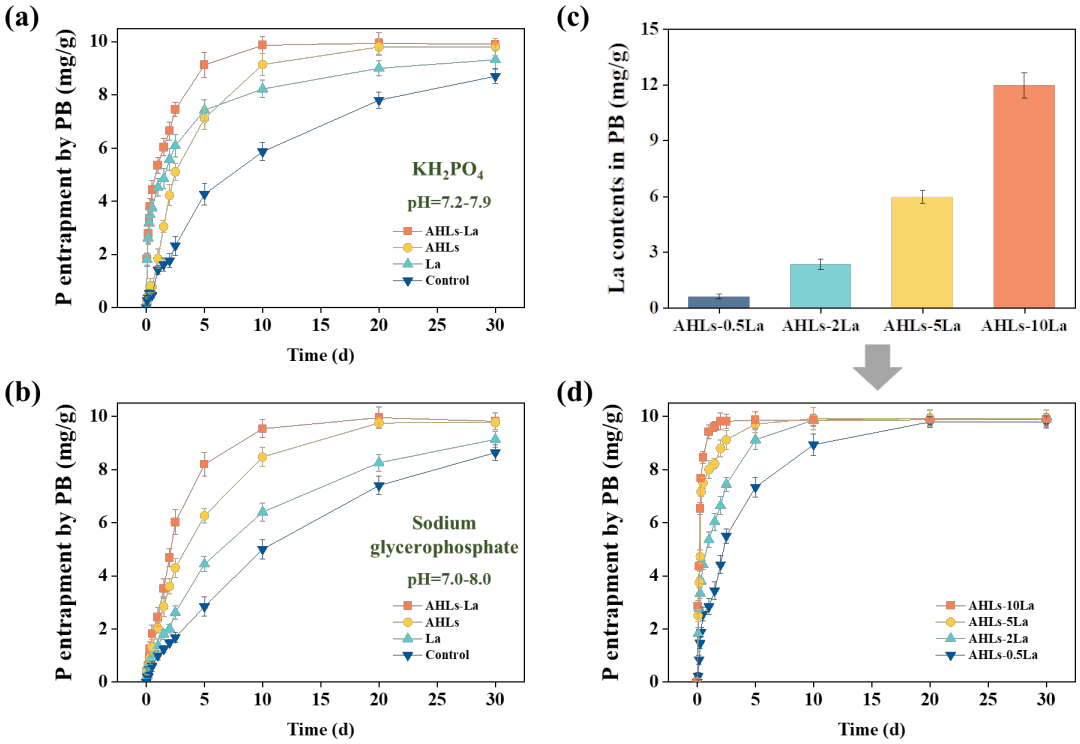
(a)
P entrapment by PB (mg/g)
Time (d)
KH2PO4
pH=7.2-7.9
AHLs-La
AHLs
La
Control
(b)
P entrapment by PB (mg/g)
Time (d)
Sodium
glycerophosphate
pH=7.0-8.0
AHLs-La
AHLs
La
Control
(c)
La contents in PB (mg/g)
AHLs-0.5La
AHLs-2La
AHLs-5La
AHLs-10La
(d)
P entrapment by PB (mg/g)
Time (d)
AHLs-10La
AHLs-5La
AHLs-2La
AHLs-0.5La

Figure 2.

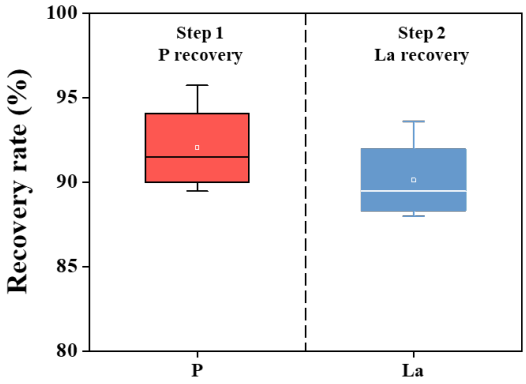
Step 1
P recovery
Step 2
La recovery
Recovery rate (%)
100
95
90
85
80
P
La

Figure 3.

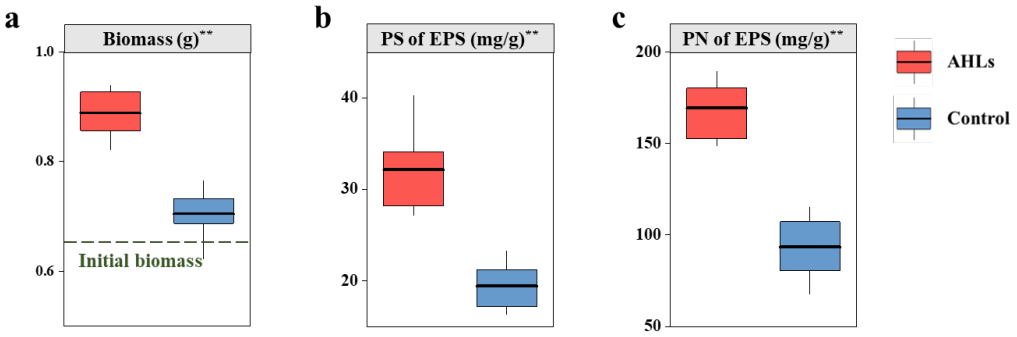

553

554 Figure 4.

555

556

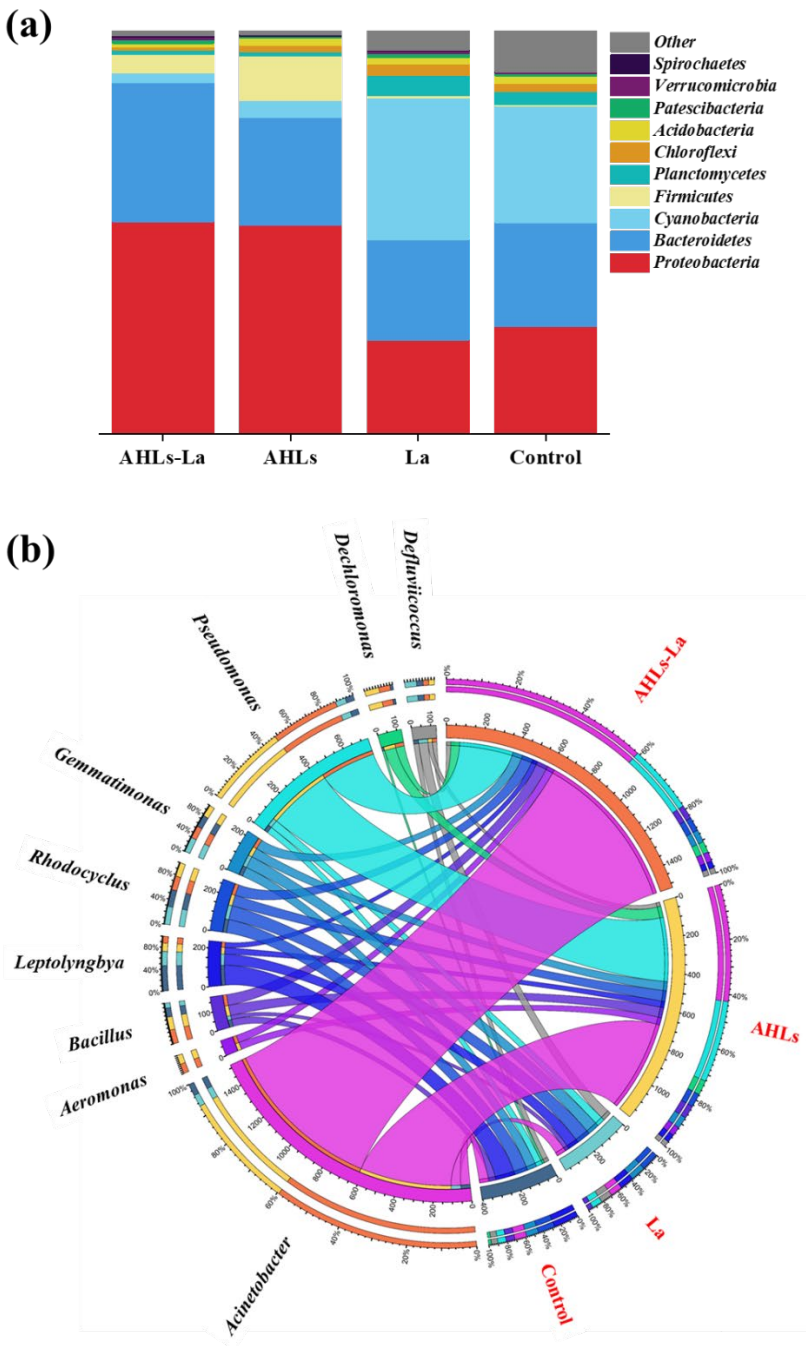
(a)
Other
Spirochaetes
Verrucomicrobia
Patescibacteria
Acidobacteria
Chloroflexi
Planctomycetes
Firmicutes
Cyanobacteria
Bacteroidetes
Proteobacteria
AHLs-La
AHLs
La
Control
(b)
Dechloromonas
Deflaviicoccus
Pseudomonas
Gemmatimonas
Rhodocyclus
Leptolyngbya
Bacillus
Aeromonas
Acinetobacter
AHLs-La
AHLs
La
Control

Figure 5.

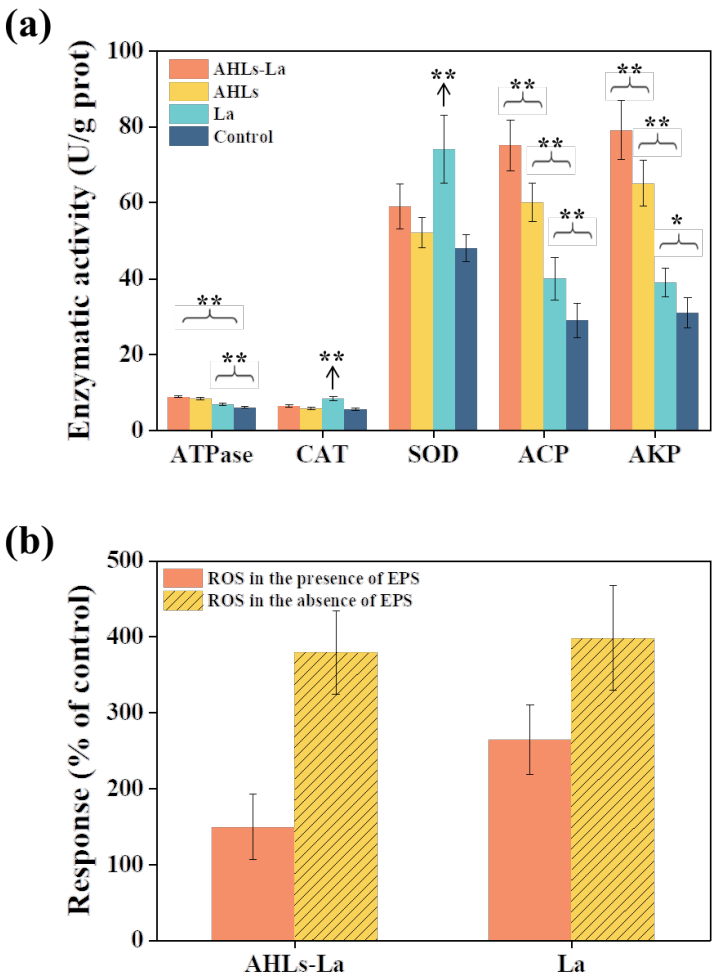

563 Figure 6.

564

565

566 Table 1. The properties of periphytic biofilm and EPS with AHLs-stimulation and La-
567 loading.

Properties		AHLs-La	AHLs	La	Control
pH		7.42±0.155	7.31±0.143	7.78±0.142	7.56±0.139
Total contents in periphytic biofilm (mg/g)[a]	La	2.86±0.181	ND	1.74±0.136	ND
	K	7.42±0.635	8.19±0.530	7.03±0.492	7.27±0.346
	Mg	2.55±0.175	2.91±0.246	1.98±0.132	2.36±0.156
	Ca	18.18±0.620	18.43±0.518	8.40±0.359	8.99±0.461
	Fe	4.71±0.523	4.96±0.711	3.81±0.214	3.93±0.247
	Al	4.07±0.332	4.84±0.262	1.95±0.194	3.03±0.267
Total contents in EPS (mg/g)[a]	La	2.16±0.112	ND	1.04±0.096	ND
	K	3.49±0.127	4.12±0.173	3.09±0.190	3.22±0.201
	Mg	0.74±0.092	0.928±0.081	0.31±0.063	0.43±0.075
	Ca	7.03±0.512	8.09±0.701	4.26±0.223	4.77±0.345
	Fe	1.47±0.082	1.95±0.065	1.09±0.012	1.44±0.078
	Al	1.09±0.011	1.72±0.012	0.67±0.009	1.30±0.020
XPS (%)	Al_2O_3	58.33 (74.3)[c]	48.12 (74.3)	58.14 (74.4)	43.81 (74.4)
	$Al(OH)_3$	41.67 (75.2)	51.88 (75.2)	41.86 (75.2)	56.19 (75.2)
	Fe_2O_3	71.60 (711.5)	40.31 (711.6)	60.92 (711.3)	47.28 (711.3)
	FeOOH	28.40 (713)	59.69 (713.6)	39.08 (713.6)	36.77 (713.4)
	Aromatic C/C-C/C-H	39.89 (284.5)	41.95 (284.9)	35.54 (284.8)	42.22 (284.7)
	C-O/aromatic C	44.51 (286)	36.96 (286.3)	45.62 (286.3)	36.36 (286.2)
	C=O/ketone C	12.15 (287.5)	14.60 (287.5)	12.95 (287.6)	15.43 (287.5)

	C in carboxylate group	3.44 (288.3)	6.49 (288.3)	5.89 (288.3)	5.98 (288.3)
	C in carbonate group	0.001 (289.2)	0.001 (289.1)	0.001 (289.2)	0.001 (289.2)

[a] n = 3; the detection limits were 0.005 mg/g for La, 0.005 mg/g for Fe, 0.020 mg/g for Al, 0.005 mg/g for Ca, 0.08 mg/g for K, and 0.002 mg/g for Mg, respectively.

[b] Not detectable.

[c] Data in parentheses show the binding energy (eV).